A single oral fixed - dose praziquantel-miltefosine nanocombination for effective control of experimental *Schistosomiasis mansoni*

Maha Mohamed Eissa
Faculty of Medicine, Alexandria University
Mervat El-Azzouni
Faculty of Medicine, Alexandria University
Labiba Khalil El-Khordagui (lakhalil@gmail.com)
Alexandria University Faculty of Pharmacy https://orcid.org/0000-0002-6607-8113
Amany Abdel Bary
Faculty of Medicine, Alexandria University
Riham Mohamed El-Moslemany
Faculty of Pharmacy, Alexandria University
Sara Ahmed Abdel Salam
Faculty of Medicine, Alexandria University

Research

Keywords: schistosomiasis mansoni, parasitic disease, preschool children, preventative care

Posted Date: February 12th, 2020

DOI: https://doi.org/10.21203/rs.2.23278/v1

Version of Record: A version of this preprint was published at Parasites & Vectors on September 15th, 2020. See the published version at https://doi.org/10.1186/s13071-020-04346-1.

Abstract

Background: Schistosomiasis control has been centered to date on praziquantel, with shortcomings involving ineffectiveness against immature worms, reinfection and emergence of drug resistance. Strategies based on drug repurposing and/or praziquantel combination therapy proved effective, though with some limitations. Combining such strategies with nanotechnology would further augment therapeutic benefits. Nanocarrier-mediated delivery of multiple drugs in schistosomiasis control has not been documented to date. Our objective was to combine drug repurposing, combinational therapy and nanotechnology for the development of a single oral fixed dose nanocombination to improve praziquantel therapeutic profile. This was based on praziquantel and an antischistosomal repurposing candidate miltefosine, co-loaded into lipid nanocapsules in reduced doses. Methods: Two fixed dose lipid nanocapsule formulations were prepared at two concentration levels of praziquantel and miltefosine. Their antischistosomal activity in comparison with control singly loaded lipoid nanocapsules was assessed in *Schistosoma mansoni*- infected mice. Single oral dos of 250mg praziquantel-20mg miltefosine/kg and 125mg praziquantel-10mg miltefosine/kg were administered on the initial day of infection, 21st and 42nd days post infection. Scanning electron microscopy, parasitological and histopathological studies were used for assessment. In vivo data were subjected to analysis of variance and post hoc test (Tukey) was used for pairwise comparisons. Results: Lipid nanocapsules showed a mean diameter of 58 nm and high entrapment efficiency of both drugs (>95%). Compared to singly loaded lipid nanocapsules, the larger dose praziquantel-miltefosine nanocombination exerted high antischistosomal efficacy in terms of % reduction of worm burden, particularly when given against invasive and juvenile worms, and amelioration of hepatic granulomas. Scanning electron microscopy revealed extensive tegumental damage with noticeable deposition of nanostructures. Conclusions: A fixed dose praziquantel-miltefosine nanocombination offers great potential as a novel single dose oral antischistosomal therapy offering multistage activity and protection against hepatic pathology. The novel drug repurposing/combination therapy/nanotechnology multiple approach has the potentials of improving the therapeutic profile of praziquantel, achieving radical cure, hindering resistance to the component drugs, and simplifying praziquantel chemotherapy. Key words: Praziquantel, miltefosine, lipid nanocapsules, *Schistosoma mansoni*, nanocombination, multistage activity, tegumental targeting, scanning electron microscopy. [LE1] [LE1]

Background

Schistosomiasis is a debilitating parasitic disease affecting more than 200 million people in over 78 tropical and sub-tropical countries, of which a significant number are preschool children (1, 2). The disease is caused by three main species of the genus Schistosoma having complex life cycles that involve an intermediate snail host and a definitive human host. S. mansoni, the causative agent of intestinal schistosomiasis, is acquired by human contact with freshwater containing infectious cercariae followed by worm migration to the mesenteric microvasculature and deposition of parasite eggs into the gut lumen. Egg deposition in the liver is associated with the formation of granulomas and subsequent

serious complications (1). In addition, both adult schistosomes and deposited eggs induce immunomodulatory effects that impair the host immune defenses against other pathogens, such as human immunodeficiency and hepatitis B/hepatitis C viruses (3, 4).

No effective vaccine exists to date and chemo-preventive therapy of schistosomiasis has relied for decades on PZQ, a low cost well tolerated drug with proven efficacy against the major species of schistosomiasis. According to the World Health Organization, PZQ is administered at the standard single oral dose of 40 mg/kg body weight in mass drug administration (MDA) programmes in endemic countries. Although such campaigns resulted in reduction of worm burden, incomplete cure attributed to ineffectiveness of PZQ against immature juvenile worms and reinfection has been reported (5, 6). Moreover, drug resistance due to the widespread use of PZQ presents a serious threat to the gains achieved (7).

Taking these concerns into consideration and given the modern resources of drug development, synthesis of PZQ derivatives (8), discovery of alternative lead compounds (9, 10), natural products (11, 12) and repurposing of existing drugs (13, 14) are effective approaches for the introduction of new antischistosomal agents. Recently, we demonstrated that MFS, a membrane active alkylphosphocholine, is a promising repurposing candidate against schistosomiasis (13, 15). The drug showed multistage activity in 5 successive 20 mg/kg/day oral doses in mice which could be significantly enhanced by lipid nanoencapsulation, allowing for a 20 mg/kg single dose oral therapy (16, 17).

Nevertheless, building on the clinical and pharmacoeconomic merits of PZQ, more success can be achieved by overcoming the main limitations of PZQ therapy. Application of new strategies such as nanotechnology and combinational therapy may extend the useful life of PZQ in more effective new formulations. In this respect, pharmaceutical nanotechnology may address challenges such as inadequate solubility, bioavailability, cellular delivery as well as nonspecific biodistribution and rapid clearance of antiparasitic drugs (18, 19). Indeed, drug delivery systems including lipid-based nanocarriers such as liposomes (20) and solid lipid nanoparticles (21), niosomes (22) and silica nanoparticles (23) were shown to enhance the bioavailability and antischistosomal activity of PZQ. Recently, we demonstrated that entrapment of PZQ into lipid nanocapsules (LNCs) significantly enhanced its antischistosomal activity in a single oral reduced dose of 250 mg/kg in mice (24). LNCs are nanostructures with great potentials in drug delivery (25–27). Owing to the their relatively small and controllable size (20–100 nm), structural integrity in simulated gastrointestinal (GI) fluids and possible active transport across the intestinal epithelium, LNCs are highly promising as oral nanovectors (28, 29). In schistosomiasis treatment, LNCs also showed potential S. mansoni tegumental targeting (24).

Apart from nanotechnology, drug combination therapy aiming at synergies, resistance reduction and rejuvenation of old drugs, is another approach showing increasing benefits in the treatment of several diseases, particularly cancer (30, 31) and bacterial infections (32). In experimental schistosomiasis, promising results have been reported for combinations involving PZQ and other drugs or biomolecules, aiming at multistage targeting, amelioration of infection-associated pathologies and resistance reduction

(12, 14). Despite evident advantages, combinations of free drugs may display variation in the pharmacokinetics and membrane transport among component drugs in addition to intricate dosing, resulting in inadequate outcomes (33). Such limitations led to the emergence of an innovative combination therapy approach based on multi-drug delivery nanocarriers with increasing benefits in diverse diseases, notably cancer (34, 35). Although still in an early stage in the treatment of infectious diseases (36), the carrier-mediated multiple drug approach proved promising in the treatment of malaria (37, 38).

To date, the research on nanocarrier-mediated drug delivery against schistosomiasis has focussed mainly on monotherapy (39). Thus, the objective of the present study was to integrate the different therapeutic benefits of PZQ and MFS with the advantages of LNCs as oral nanocarrier with demonstrated schistosome tegumental targeting in a multifunctional single oral fixed dose nanocombination in experimental schistosomiasis mansoni in mice. The antischistosomal efficacy of two fixed dose nanocombinations with two dosing levels of both drugs was assessed against different developmental stages of the parasite using SEM, parasitological parameters and histopathological examination.

Methods

Materials

PZQ (Gift of the Egyptian International Pharmaceuticals Industries Company (EIPICO), Cairo, Egypt), MFS (Chem-Impex International, New York, USA), Labrafac® lipophile WL 1349 (Gattefossé SA, Saint-Priest, France), Kolliphor HS 15 (BASF, Ludwigshafen, Germany), Lipoid S100 (a soybean lecithin containing 94% of phosphatidylcholine, Lipoïd GMBH, Ludwigshafen, Germany), Oleic acid (OA, Sigma-Aldrich Co., St Louis, MO, USA), acetonitrile HPLC grade (Thermo Fisher Scientific, Waltham, MA, USA), Span® 80 (LobaChemie for Laboratory Reagents and Fine Chemicals, Mumbai, India). All other chemicals were of analytical grade.

Formulation and characterization of lipid nanocapsules

LNCs were formulated with oleic acid and Span 80 and prepared by the phase inversion method (24, 27). In brief, Kolliphor® HS 15, Labrafac lipophile WL 1349 and deionized water containing NaCl (0.88% w/w of the final dispersion) were weighed and mixed using a magnetic stirrer in the ratio 5:6:9. Span 80 (2% w/w) and oleic acid (6 % w/w) were added to the primary mixture which was subjected to three progressive heating and cooling cycles between 45-75°C at 4°C/min. An irreversible shock was induced by two-fold dilution with cold deionized water (0-2°C) added to the formed o/w emulsion at a temperature 1-3°C from the beginning of the phase inversion zone. This was followed by slow magnetic stirring at room temperature for five min. For the preparation of drug loaded LNCs, PZQ was added to the primary mixture of ingredients at concentrations 25 or 12.5 mg/ml, whereas MFS was added just before quenching at a concentration of 2 or 1 mg/ml of the final dispersion. The procedure was used to prepare a higher fixed dose combination containing 25 mg PZQ and 2 mg MFS/ml of dispersion and a lower fixed dose combination containing 12.5 mg PZQ and 1 mg MFS/ml of dispersion and their corresponding

singly loaded counterparts, PZQ 25 mg/ml, MFS 2 mg/ml, PZQ 12.5 mg/ml and MFS 1 mg/ml. The fixed dose combination LNC dispersions were used in calculated volumes to provide a dose of 250 mg/kg PZQ-20 mg/kg MFS and 125 mg/kg PZQ-10 mg/kg MFS respectively in the antischistosomal study in mice.

LNC formulations were characterized for morphology, colloidal properties and drug entrapment efficiency (EE%). The morphology of LNCs was examined by transmission electron microscopy (TEM) using JEOL, JEM-100 CX Electron Microscope, Tokyo, Japan. Before analysis, the LNC dispersion was treated with 2% w/v uranyl acetate solution as a negative stain and sprayed onto copper grids. Shots were taken at X 7500 at 80 kV. The average particle size, polydispersity index (PdI) and zeta potential (ZP) were measured by photon correlation spectroscopy (PCS) at a fixed angle 173° using a 4 mW He-Ne laser at 25ºC. The EE% was obtained by determining the concentration of free (unentrapped) PZQ and MFS in the ultrafiltrate after separation of LNCs using an ultrafiltration/centrifugation technique. The concentration of unentrapped PZQ in the ultrafiltrate was determined by HPLC-UV as reported (24). MFS concentration was measured by a modified spectrophotometric assay originally reported for quaternary ammonium compounds and validated for MFS quantitation (16).

Antischistosomal efficacy in mice

Schistosoma mansoni infection of animals

The life cycle of *S. mansoni* was maintained in the Medical Parasitology Department, Faculty of Medicine, Alexandria University by serial passages in laboratory-bred Biomphalaria *alexandrina* snails and Swiss strain albino mice as reported . A total of 128 mice, six to eight weeks old, weighing 20-30 gram each, were obtained from the animal house of the Medical Parasitology Department, Faculty of Medicine, Alexandria University. Mice were housed under specific pathogen-free barrier conditions. Each mouse was infected with 100 ±10 freshly shed cercariae using the paddling technique (40). All mice were subjected to infection.

Animal groups

One hundred and twenty-eight mice were allocated to a nontreated control group (NT) including 8 mice and 2 experimental groups, Group I and Group II, 60 mice each.

Group I: subdivided into 3 subgroups 20 mice each and treated with LNC dispersions corresponding to the required dose of the higher fixed dose nanocombination or its singly loaded counterpart controls as follows:

Subgroup Ia: PZQ 250 mg/kg

Subgroups Ib: MFS 20 mg/kg

Subgroup Iab: PZQ 250 mg-MFS 20 mg /kg

Group II: subdivided into 3 subgroups 20 mice each and treated with LNC dispersions corresponding to the required dose of the lower fixed dose nanocombination or its singly loaded counterpart controls as follows:

Subgroup IIa: PZQ 125 mg/kg

Subgroup IIb: MFS 10 mg/kg

Subgroup IIab: PZQ 125-MFS 10mg /kg.

Mice in all treated subgroups (Ia, Ib and Iab, IIa, IIb and IIab) were administered a calculated volume of the LNCs dispersion corresponding to the required dose of the PZQ-MFS fixed dose combinations or the corresponding singly loaded LNCs by gastric gavage. Mice in these groups were further subdivided into three subgroups (1, 2, 3) which were given a single oral dose of the drug(s) nanoformulations at three different dates (on the initial day of infection, 21st and 42nd days p.i.) corresponding to the three stages of *S. mansoni* life cycle (invasive, juvenile and adult stages (41). The number of mice/ group treated on the initial day of infection and 21st day p.i. (against invasive and immature stages) was six whereas, it was eight for all other subgroups treated on the 42nd day p.i. (against the adult stage). Two infected mice treated on the 42nd day p.i. were sacrificed 24 h after administration of the nanoformulations to collect the adult worms for morphological examination using SEM (Jeol JSM- IT200, Jeol, Tokyo, Japan). The remaining mice of all subgroups were sacrificed on the 49th day p.i. The therapeutic efficacy of the two fixed dose nanocombinations in comparison with the corresponding singly loaded control LNCs and the nontreated control was assessed by determination of the percentage reduction in total worm burden, the size of hepatic granulomas, histopathological changes in liver parenchyma and examination of the morphology of recovered worms by SEM.

Antischistosomal activity assessment

Morphological examination by scanning electron microscopy

Adult worms were recovered 24 h post administration of nanoformulations from two infected mice from all subgroups treated on the 42nd day p.i. against the adult stage for SEM imaging. Worms were fixed in cold 2.5% buffered glutaraldehyde phosphate (pH 7.4), processed, examined under SEM and photographed (42).

Estimation of adult worm burden

On the 49th day p.i., adult worms were recovered from the hepatic and mesenteric vessels from mice in all study groups using the perfusion technique (40).

Histopathological examination

Specimens of the liver of mice of all study groups were fixed in 10% neutral buffered formalin. Histological sections, 5 µm-thick, were stained with hematoxylin and eosin (H&E). Pathological changes in the hepatic parenchyma were observed and the mean size of granulomas was determined. Only granulomas containing one central clearly identifiable egg were selected (43).

Statistical analysis

Data were analyzed using IBM SPSS software package version 20.0 (Armonk, NY: IBM Corp). Kolmogorov-Smirnov test was used to verify the normality of distribution. Quantitative data were described using mean and standard deviation. Significance of the obtained results was judged at the 5% level. For normally distributed quantitative variables, F-test (ANOVA) was used to compare between more than two groups and Post Hoc test (Tukey) was used for pairwise comparisons. The percentage reduction (% R) of the adult worm load as well as the granuloma size were calculated as follows:

$$\text{Percentage reduction (\% R)} = \frac{N - n}{N} \times 100$$

Where, (N) is the mean number of worms or the mean granuloma size in the infected nontreated group and (n) is the mean number of worms or the mean granuloma size in the infected treated subgroups.

Results

Characterization of lipid nanocapsules

As indicated by SEM imaging (Fig. 1), sample PZQ-MFS combination LNCs were in the nano size range, almost spherical, homogenously distributed and not aggregated. LNCs were generally monodisperse with a PdI not exceeding 0.05. Blank LNCs had a mean diameter of 52.22±0.42 nm with a ZP of -6.5±0.4 mV. Drug loading into LNCs slightly but significantly affected their colloidal properties (57.61±0.15 nm and -7.9±0.4 mV). The EE% values exceeded 97% for both PZQ and MFS.

Antischistosomal activity in *S. mansoni*-infected mice

Morphological properties by SEM

Results of the SEM examination are shown in Fig. 2. SEM images of normal *S. mansoni* male worms recovered from infected non-treated mice (NT) (Fig. 2A), showed round to oval oral and ventral suckers (Fig. 2B) with apically directed spines (Fig. 2C). The dorsolateral tegumental surface of the mid-body showed crablike uniformly distributed tubercles that had sharp visible intact spines and sensory papillae (Fig. 2D). The tegument between the tubercles showed ridges (Fig. 2E). On the other hand, male worms recovered from *S. mansoni*-infected mice treated with the higher dose PZQ-MFS nanocombination (PZQ 250 mg-MFS 20 mg/kg, Subgroup Iab) showed deformity in the whole body (Fig. 2F) as well as in the oral and ventral suckers (Fig. 2G), with blunt, short and loose spines (Fig. 2H). There was extensive dorsal

tegumental damage in the form of peeling of tubercles and spine disfigurement (Fig. 2I) with appearance of subtegumental tissues. Marked deposition of nanostructures of the size of LNCs on the damaged tegument (Fig. 2J) and on the loose disfigured spines (Fig. 2K) was observed. The tegumental changes and sucker's deformity observed in infected mice treated with either PZQ 250 mg/kg or MFS 20 mg/kg monotherapy (control Subgroups Ia and Ib respectively) were almost similar. Comparable but milder morphological changes were also observed in worms recovered from infected mice treated with the lower dose PZQ-MFS LNCs combination PZQ 125 mg-MFS 10 mg/kg (Subgroup IIab) and the corresponding singly loaded LNCs (control Subgroups IIa and IIb).

Assessment of adult worm burden

Data for worm burden assessment in the study groups are shown in Table 1. Oral administration of the two fixed dose combinations of PZQ-MFS LNCs (Subgroups Iab1,2,3 and IIab1,2,3) to infected mice resulted in statistically significant reduction in the mean adult worm burden compared to the infected nontreated control and their corresponding singly loaded control LNCs (Subgroups Ia1 and Ia2 and subgroups IIa2 and IIb1,3 respectively). There was also a statistically significant difference of worm burden between the two fixed dose nanocombinations (subgroups Iab and IIab) in favour of the higher dose combination (subgroup Iab) against the three different developmental stages (Subgroup Ia1,2,3) ($p \leq 0.05$).

Assessment of histopathological changes in the liver

As shown in Fig. 3, the histopathological changes detected in H&E-stained liver sections of infected nontreated mice showed preserved hepatic architecture associated with granulomatous reaction located perivascularly and intraparenchymally (Fig. 3A). Most of the detected granulomas were active and formed mainly of eosinophils, lymphocytes and histocytes encircling laid *S. mansoni* eggs (Fig. 3B). There was deposition of bilharzial pigments (Fig. 3C), Kupffer cells hyperplasia (Fig. 3D), and fatty changes in hepatocytes (Fig. 3E).

On the other hand, pronounced amelioration of *S. mansoni*-associated hepatic pathology was observed in all developmental stages in infected mice treated with the higher dose nanocombination (subgroup Iab1,2,3), manifested as scanty small healed granulomas formed of minimal inflammatory cellular infiltration and surrounded by concentric collagenous fibrous tissue (Fig. 3F). Marked improvement of hepatic pathology was also observed in all infected mice treated with singly loaded control LNCs at the higher dosing level (Subgroups Ia1,2,3 and Ib1,2,3). On the other hand, only minimal improvement in infection-associated hepatic pathological changes was observed in all infected mice treated with the lower dose nanocombination (Subgroups IIab1,2,3) as well as their corresponding singly loaded control LNCs (Subgroups IIa1,2,3 and IIb1,2,3).

As regards hepatic granulomas, results listed in Table 2 indicated that the highest statistically significant reduction in mean granulomas size was observed in infected mice treated with the higher dose nanocombination (subgroup Iab1,2,3) as compared to the infected nontreated control, their

corresponding singly loaded control LNCs (Subgroup Ia2,3 and Subgroup Ib3) as well as the lower dose nanocombination (subgroup IIa1,2,3) ($p \leq 0.05$).

Discussion

We aimed at improving the antischistosomal therapeutic profile of PZQ in MDA programmes by enhancing multistage activity against the different developmental stages of the parasite, alleviating schistosomiasis-induced pathology and potentially reducing drug resistance while keeping dosage at a relatively low single oral dose. This could not be achieved unless multiple strategies are exploited. In this study, an innovative approach based on the integration of documented benefits of three strategies, namely drug repurposing, combination of multi-target drugs and nanotechnology, in developing PZQ LNCs incorporating MFS in a nanocombination intended for single dose oral therapy of schistosomiasis mansoni with the least effective doses.

As the key combination drug, PZQ exerts a direct antischistosomal effect on adult worms by underpinning the parasite Ca 2 + homeostasis resulting in spastic paralysis and rapid vacuolization of the worm surface (44). Recently, activation of a schistosome transient receptor potential channel by PZQ was shown to support the pharmacological profile of PZQ (45). To overcome the known shortcomings of PZQ therapy, mainly ineffectiveness against immature worms and inability to ameliorate disease-associated pathology, MFS was included in the nanocombination. Selection of MFS relied on its current clinical use as the only approved oral drug for the treatment of visceral leishmaniasis (46) as well as earlier evidence of multistage antischistosomal activity of oral MFS in mice (13). Although the antischistosomal mechanism of activity of MFS is not well established yet, antiparasitic and anticancer effects of MFS appear to be related to its high affinity for plasma membrane (47, 48). As a membrane active zwitterionic alkylphospholipid, MFS causes dramatic increases in membrane dynamics by interacting with the protein component and inhibiting phospholipid turnover and lipid-dependent cell signaling pathways, leading to apoptosis. Of importance to schistosomiasis, MFS impedes the biosynthesis of sphingomyelin, a schistosome membrane phospholipid which hides the surface membrane proteins from the host immune system (49). Evident damage to the Schistosoma tegument with exposure of their surface antigens was reported following treatment with MFS (13, 16, 50).

Selection of LNCs as nanocarrier for the oral administration of the PZQ-MFS combination was based primarily on its recognized merits as lipid-based nanocarrier for oral drug delivery with modifiable composition. For example, LNCs were demonstrated to enhance the activity of MFS against S. mansoni compared to the free drug (67.51 and 8.13% reduction in worm burden respectively) with further enhancement (88.46% reduction) upon modification of LNCs with oleic acid as membrane permeabilizer (16). Owing to its amphiphilic nature, MFS molecules are possibly intercalated within the tensioactive shell of LNCs, enhancing their structural integrity allowing for potential translocation across the intestinal membrane. A hypothesized structure of MFS-LNCs has been reported earlier (16). LNCs modified with oleic acid and MFS as formulation additives also enhanced the activity of PZQ against experimental

schistosomiasis mansoni (24). In both MFS and PZQ systems, LNCs allowed marked sustained release of the active drugs for at least 24 h.

Analysis of data obtained in the present study indicated that the activity of PZQ LNCs (250 mg/kg) against schistosomiasis mansoni was in the order of adult > invasive > juvenile while that of MFS LNCs (20 mg/kg) was in the order of juvenile > adult > invasive corroborating literature data for both drugs in the free form (13, 51, 52) and nanoencapsulated form (17, 24). The nanocombination of MFS with PZQ in the same doses (PZQ 250 mg/kg-MFS 20 mg/kg) resulted in high activity against pre-patent and patent infection implying multistage activity, a main objective of the present study.

Significant reduction in mean adult worm burden (Table 1), liver granuloma size (Table 2) in addition to the amelioration of hepatic pathology (Fig. 3) were obvious in the higher dose nanocombination-treated group (Group Iab) compared to the infected nontreated control and the respective singly loaded PZQ (Subgroup Ia) or MFS (Subgroup Ib) control LNCs. This denoted greater amelioration of schistosomiasis-induced pathology which results from immune-mediated granulomatous responses against Schistosoma eggs trapped in tissues. These are likely to cause serious local and systemic pathological effects associated with granuloma formation and fibrosis (53). The significant reduction in hepatic granuloma size could be attributed to the distribution of PZQ (13, 54) and MFS (55, 56) to the liver of mice. Hepatic granulomas shrink progressively after PZQ treatment as a result of schistosome killing and reduction in the number of eggs trapped in the liver, reversing fibrogenesis (57).

In addition, suckers and teguments of adult male schistosomes recovered from S. mansoni-infected mice in the higher dose nanocombination subgroup (Iab) showed deformed suckers as well as extensive tegumental damage in the form of peeling of tubercles, disfigurement of spines and appearance of subtegumental tissue (Fig. 2) supporting earlier observations for singly loaded PZQ LNCs (24) and MFS LNCs (16). Suckers promote the attachment of schistosomes to blood vessels for the feeding process (1). The tegument of Schistosoma also plays an important role in the uptake of nutrients and ions, excretion of metabolic end products as well as protection against the host immunological attack (58).

The obvious change observed in the therapeutic profile of nanoencapsulated PZQ induced by the addition of MFS in the higher dose nanocombination pointed to the benefit of combining drugs having different modes of action in appropriate dosing. This substantiated literature data for antischistosomal combinational therapies based exclusively on free drugs to date. Examples of PZQ combinations with enhanced efficacy in terms of reduced worm burden, or protection against pathological sequelae or multistage activity include PZQ-artesunate (59), PZQ-resveratrol-N-acetylcysteine (60), PZQ-edelfosine (61) and PZQ-natural products (12, 62). However, the fear of development of Plasmodium resistance to antimalarials and the relatively long treatment duration required for other combinations may hinder their applicability. This highlights the benefit of the current single oral dose nanoformulation.

Another great advantage of antischistosomal LNC formulations is their tegumental targeting ability observed earlier for MFS LNCs modified with oleic acid (16) and PZQ LNCs modified with oleic acid and a low concentration of MFS as formulation additives (16, 24). Such observations have been substantiated

in the present by high magnification SEM visualization of nano-objects of the size of LNCs deposited on the damaged tegument and the loose disfigured spines of adult S. mansoni worms (Fig. 2J&K). This also emphasizes the role of oral nanocarriers in mediating cellular drug delivery, providing new avenues for modified therapies (63).

A further objective of the study was to keep the doses of PZQ and MFS at the lowest level for effective therapy. Although the amounts of PZQ and MFS entrapped in the higher dose PZQ-MFS nanocombination were already reduced relative to the free drug forms (16, 43), an attempt was made to assess the effect of halving the dose of both drugs on the combined antischistosomal activity of a second lower dose fixed dose nanocombination using the same procedures (Tables 1 and 2, Group II). Results indicated a statistically significant reduction in the antischistosomal activity of the lower dose nanocombination and its singly loaded control counterparts denoting ineffectiveness of the half dose nanocombination.

Based on the results obtained, the antischistosomal activity of PZQ as the gold standard of antischistosomal therapy to date could be significantly enhanced by utilizing a multiple approach based on drug combination, drug repurposing and nanotechnology. Interaction of the nanocombination components resulted in the great promises offered by the higher dose PZQ-MFS nanocombination developed in the study. These include high efficacy against experimental schistosomiasis mansoni at the reduced doses of 250 mg/kg of PZQ and 20 mg/kg of MFS compared to singly loaded control LNCs and the lower dose nanocombination. Efficacy enhancement was verified by a multistage activity of the PZQ-MFS LNCs bestowed by the repurposing candidate MFS which also contributes to the structural stability and membrane activity of LNCs, probably facilitating tegumental targeting. Moreover, a statistically significant reduction in the size of hepatic granulomas, implied amelioration of a serious disease-associated liver pathology. Finally, a rationally selected nanocarrier (oleic-acid modified LNCs) showing controlled drug delivery and great benefits in oral administration contributed to efficacy enhancement by facilitating the intestinal translocation of the nanocombination and tegumental targeting.

Conclusion

The concept of PZQ-MFS nanocombinational therapy that may lead to a wide antischistosomal therapeutic profile capable of achieving radical cure and hinderance of resistance to both component drugs. The use of such a fixed dose combination therapy is cost effective and has the advantage of simplifying the medication regimen, improving patient compliance and clinical outcomes. To the best of our knowledge, this is the first report of a fixed dose nano-based combinatorial therapy for schistosomiasis mansoni. The concept can be explored for novel drug formulations for other neglected infectious diseases. Further studies are in progress to assess the safety and prophylactic efficacy of the PZQ-MFS nanocombination.

Abbreviations

EE%
entrapment efficiency
GI
gastrointestinal
H&E
hematoxylin and eosin
LNCs
lipid nanocapsules
MDA
mass drug administration
MFS
miltefosine
PCS
photon correlation spectroscopy
PdI
polydispersity index
p.i.
postinfection
PZQ
praziquantel
S.
Schistosoma
SEM
scanning electron microscopy
TEM
transmission electron microscopy
ZP
zeta potential

Declarations

Ethics approval and consent to participate

The study protocol was approved by the Ethics Committee of the Faculty of Medicine, Alexandria University, based on Egyptian regulations for animal experimentation (Protocol approval number: 0201101).

Consent for publication

Not applicable.

Availability of data and materials

The data supporting the conclusions of this article are provided within the article.

Competing interests

The authors declare that they have no competing interests.

Funding

The authors received no specific funding for this work.

Authors' contributions

MME and LEK conceived the study. MME, MZE and SAA designed the study. LKE and RME formulated and characterized the lipid nanocapsules. SAA and RME conducted the experiments. MME, MZE and SAA performed the SEM study. AA and SAA performed the histopathological study. MZE, LEK and SAA performed the data analysis. MME, MZE, LEK, AA, RME and SAA prepared the figures and tables. MME, LEK and SAA wrote the manuscript. All authors read and approved the final manuscript**.**

Acknowledgements

The authors are grateful to Mrs Dawlat Ahmed for technical assistance with animal experimentation.

Authors information

1 Department of Medical Parasitology, Faculty of Medicine, Alexandria University, Egypt.

2 Department of Pharmaceutics, Faculty of pharmacy, Alexandria University, Egypt.

3 Department of Pathology, Faculty of Medicine, Alexandria University, Egypt.

References

1. LoVerde PT. Schistosomiasis. In: Toledo R, Fried B, editors. Digenetic Trematodes. Cham: Springer International Publishing; 2019. p. 45-70.
2. Osakunor DN, Woolhouse ME, Mutapi F. Paediatric schistosomiasis: What we know and what we need to know. PLoS neglected tropical diseases. 2018;12(2):e0006144.
3. Wall KM, Kilembe W, Vwalika B, Dinh C, Livingston P, Lee Y-M, et al. Schistosomiasis is associated with incident HIV transmission and death in Zambia. PLoS neglected tropical diseases. 2018;12(12):e0006902.
4. Omar HH. Impact of chronic schistosomiasis and HBV/HCV co-infection on the liver: current perspectives. Hepatic Medicine: Evidence and Research. 2019;11:131.
5. Woldegerima E, Bayih AG, Tegegne Y, Aemero M, Jejaw Zeleke A. Prevalence and Reinfection Rates of Schistosoma mansoni and Praziquantel Efficacy against the Parasite among Primary School

Children in Sanja Town, Northwest Ethiopia. J Parasitol Res. 2019;2019.

6. Black CL, Steinauer ML, Mwinzi PN, Evan Secor W, Karanja DM, Colley DG. Impact of intense, longitudinal retreatment with praziquantel on cure rates of schistosomiasis mansoni in a cohort of occupationally exposed adults in western Kenya. Tropical Medicine & International Health. 2009;14(4):450-7.
7. Vale N, Gouveia MJ, Rinaldi G, Brindley PJ, Gartner F, Correia da Costa JM. Praziquantel for Schistosomiasis: Single-Drug Metabolism Revisited, Mode of Action, and Resistance. Antimicrobial agents and chemotherapy. 2017;61(5).
8. da Silva VBR, Boucherle B, El-Methni J, Hoffmann B, da Silva AL, Fortune A, et al. Could we expect new praziquantel derivatives? A meta pharmacometrics/pharmacoinformatics analysis of all antischistosomal praziquantel derivatives found in the literature. SAR QSAR Environ Res. 2019;30(6):383-401.
9. Lyu H, Petukhov PA, Banta PR, Jadhav A, Lea W, Cheng Q, et al. Characterization of lead compounds targeting the selenoprotein thioredoxin glutathione reductase for treatment of schistosomiasis. ACS Infect Dis. 2020.
10. Saccoccia F, Brindisi M, Gimmelli R, Relitti N, Guidi A, Saraswati AP, et al. Screening and Phenotypical Characterization of Schistosoma mansoni Histone Deacetylase 8 (SmHDAC8) Inhibitors as Multistage Antischistosomal Agents. ACS Infect Dis. 2020;6(1):100-13.
11. Abou El Dahab MM, Shahat SM, Mahmoud SSM, Mahana NA. In vitro effect of curcumin on Schistosoma species viability, tegument ultrastructure and egg hatchability. Experimental parasitology. 2019;199:1-8.
12. Beshay EVN, Rady AA, Afifi AF, Mohamed AH. Schistosomicidal, antifibrotic and antioxidant effects of Cucurbita pepo L. seed oil and praziquantel combined treatment for Schistosoma mansoni infection in a mouse model. J Helminthol. 2019;93(3):286-94.
13. Eissa MM, El-Azzouni MZ, Amer EI, Baddour NM. Miltefosine, a promising novel agent for schistosomiasis mansoni. International journal for parasitology. 2011;41(2):235-42.
14. Gouveia MJ, Brindley PJ, Gartner F, Costa J, Vale N. Drug Repurposing for Schistosomiasis: Combinations of Drugs or Biomolecules. Pharmaceuticals (Basel). 2018;11(1).
15. Eissa MM, El Bardicy S, Tadros M. Bioactivity of miltefosine against aquatic stages of Schistosoma mansoni, Schistosoma haematobium and their snail hosts, supported by scanning electron microscopy. Parasites & vectors. 2011;4:73.
16. Eissa MM, El-Moslemany RM, Ramadan AA, Amer EI, El-Azzouni MZ, El-Khordagui LK. Miltefosine Lipid Nanocapsules for Single Dose Oral Treatment of Schistosomiasis Mansoni: A Preclinical Study. PloS one. 2015;10(11):e0141788.
17. El-Moslemany RM, Eissa MM, Ramadan AA, El-Khordagui LK, El-Azzouni MZ. Miltefosine lipid nanocapsules: Intersection of drug repurposing and nanotechnology for single dose oral treatment of pre-patent schistosomiasis mansoni. Acta tropica. 2016;159:142-8.

18. Santos-Valle ABC, Souza GR, Paes CQ, Miyazaki T, Silva AH, Altube MJ, et al. Nanomedicine strategies for addressing major needs in neglected tropical diseases. Annual Reviews in Control. 2019.
19. Sun Y, Chen D, Pan Y, Qu W, Hao H, Wang X, et al. Nanoparticles for antiparasitic drug delivery. Drug Deliv. 2019;26(1):1206-21.
20. Labib El Gendy AEM, Mohammed FA, Abdel-Rahman SA, Shalaby TIA, Fathy GM, Mohammad SM, et al. Effect of nanoparticles on the therapeutic efficacy of praziquantel against Schistosoma mansoni infection in murine models. Journal of parasitic diseases : official organ of the Indian Society for Parasitology. 2019;43(3):416-25.
21. Radwan A, El-Lakkany NM, William S, El-Feky GS, Al-Shorbagy MY, Saleh S, et al. A novel praziquantel solid lipid nanoparticle formulation shows enhanced bioavailability and antischistosomal efficacy against murine S. mansoni infection. Parasites & vectors. 2019;12(1):304.
22. Zoghroban HS, El-Kowrany SI, Aboul Asaad IA, El Maghraby GM, El-Nouby KA, Abd Elazeem MA. Niosomes for enhanced activity of praziquantel against Schistosoma mansoni: in vivo and in vitro evaluation. Parasitology research. 2019;118(1):219-34.
23. Tawfeek GM, Baki MHA, Ibrahim AN, Mostafa MAH, Fathy MM, Diab M. Enhancement of the therapeutic efficacy of praziquantel in murine Schistosomiasis mansoni using silica nanocarrier. Parasitology research. 2019.
24. Amara RO, Ramadan AA, El-Moslemany RM, Eissa MM, El-Azzouni MZ, El-Khordagui LK. Praziquantel-lipid nanocapsules: an oral nanotherapeutic with potential Schistosoma mansoni tegumental targeting. Int J Nanomedicine. 2018;13:4493-505.
25. Carradori D, Labrak Y, Miron VE, Saulnier P, Eyer J, Preat V, et al. Retinoic acid-loaded NFL-lipid nanocapsules promote oligodendrogenesis in focal white matter lesion. Biomaterials. 2020;230:119653.
26. Fabbri J, Espinosa JP, Pensel PE, Medici SK, Gamboa GU, Benoit JP, et al. Do albendazole-loaded lipid nanocapsules enhance the bioavailability of albendazole in the brain of healthy mice? Acta tropica. 2020;201:105215.
27. Huynh NT, Passirani C, Saulnier P, Benoit JP. Lipid nanocapsules: a new platform for nanomedicine. International journal of pharmaceutics. 2009;379(2):201-9.
28. Ullio Gamboa GV, Pensel PE, Elissondo MC, Sanchez Bruni SF, Benoit JP, Palma SD, et al. Albendazole-lipid nanocapsules: Optimization, characterization and chemoprophylactic efficacy in mice infected with Echinococcus granulosus. Experimental parasitology. 2019;198:79-86.
29. Varshosaz J, Taymouri S, Jahanian-Najafabadi A, Alizadeh A. Efavirenz oral delivery via lipid nanocapsules: formulation, optimisation, and ex-vivo gut permeation study. IET Nanobiotechnol. 2018;12(6):795-806.
30. Derakhshani A, Rezaei Z, Safarpour H, Sabri M, Mir A, Sanati MA, et al. Overcoming trastuzumab resistance in HER2-positive breast cancer using combination therapy. J Cell Physiol. 2020;235(4):3142-56.

31. Kawazoe A, Shitara K. Trifluridine/tipiracil for the treatment of metastatic gastric cancer. Expert Rev Gastroenterol Hepatol. 2020:1-6.
32. Coates ARM, Hu Y, Holt J, Yeh P. Antibiotic combination therapy against resistant bacterial infections: synergy, rejuvenation and resistance reduction. Expert Rev Anti Infect Ther. 2020;18(1):5-15.
33. Hu CM, Aryal S, Zhang L. Nanoparticle-assisted combination therapies for effective cancer treatment. Therapeutic delivery. 2010;1(2):323-34.
34. Al-Attar T, Madihally SV. Recent advances in the combination delivery of drug for leukemia and other cancers. Expert Opin Drug Deliv. 2020.
35. Zhao M, van Straten D, Broekman MLD, Preat V, Schiffelers RM. Nanocarrier-based drug combination therapy for glioblastoma. Theranostics. 2020;10(3):1355-72.
36. Walvekar P, Gannimani R, Govender T. Combination drug therapy via nanocarriers against infectious diseases. European Journal of Pharmaceutical Sciences. 2019;127:121-41.
37. Lingani M, Bonkian LN, Yerbanga I, Kazienga A, Valea I, Sorgho H, et al. In vivo/ex vivo efficacy of artemether-lumefantrine and artesunate-amodiaquine as first-line treatment for uncomplicated falciparum malaria in children: an open label randomized controlled trial in Burkina Faso. Malar J. 2020;19(1):8.
38. Mathenge PG, Low SK, Vuong NL, Mohamed MYF, Faraj HA, Alieldin GI, et al. Efficacy and resistance of different artemisinin-based combination therapies: a systematic review and network meta-analysis. Parasitol Int. 2020;74:101919.
39. Tomiotto-Pellissier F, Miranda-Sapla MM, Machado LF, Bortoleti B, Sahd CS, Chagas AF, et al. Nanotechnology as a potential therapeutic alternative for schistosomiasis. Acta tropica. 2017;174:64-71.
40. Smithers SR, Terry RJ. The infection of laboratory hosts with cercariae of Schistosoma mansoni and the recovery of the adult worms. Parasitology. 1965;55(4):695-700.
41. El-Moslemany RM, Eissa MM, Ramadan AA, El-Khordagui LK, El-Azzouni MZ. Miltefosine lipid nanocapsules: intersection of drug repurposing and nanotechnology for single dose oral treatment of pre-patent schistosomiasis mansoni. Acta tropica. 2016;159:142-8.
42. Jeffree CE, Read ND. Ambient-and low-temperature scanning electron microscopy. Electron microscopy of plant cells. 1991;313:413.
43. Amara RO, Ramadan AA, El-Moslemany RM, Eissa MM, El-Azzouni MZ, El-Khordagui LK. Praziquantel–lipid nanocapsules: an oral nanotherapeutic with potential Schistosoma mansoni tegumental targeting. International journal of nanomedicine. 2018;13:4493.
44. Chan JD, Zarowiecki M, Marchant JS. Ca2+ channels and praziquantel: a view from the free world. Parasitology international. 2013;62(6):619-28.
45. Park SK, Gunaratne GS, Chulkov EG, Moehring F, McCusker P, Dosa PI, et al. The anthelmintic drug praziquantel activates a schistosome transient receptor potential channel. J Biol Chem. 2019;294(49):18873-80.

46. Monge-Maillo B, Lopez-Velez R. Miltefosine for visceral and cutaneous leishmaniasis: drug characteristics and evidence-based treatment recommendations. Clinical infectious diseases : an official publication of the Infectious Diseases Society of America. 2015;60(9):1398-404.
47. Fernandes KS, de Souza PE, Dorta ML, Alonso A. The cytotoxic activity of miltefosine against Leishmania and macrophages is associated with dynamic changes in plasma membrane proteins. Biochim Biophys Acta Biomembr. 2017;1859(1):1-9.
48. Moreira RA, Mendanha SA, Fernandes KS, Matos GG, Alonso L, Dorta ML, et al. Miltefosine increases lipid and protein dynamics in Leishmania amazonensis membranes at concentrations similar to those needed for cytotoxicity activity. Antimicrobial agents and chemotherapy. 2014;58(6):3021-8.
49. El Ridi R, Tallima H. Equilibrium in lung schistosomula sphingomyelin breakdown and biosynthesis allows very small molecules, but not antibody, to access proteins at the host–parasite interface. Journal of Parasitology. 2006;92(4):730-7.
50. Bertao HG, da Silva RA, Padilha RJ, de Azevedo Albuquerque MC, Radis-Baptista G. Ultrastructural analysis of miltefosine-induced surface membrane damage in adult Schistosoma mansoni BH strain worms. Parasitology research. 2012;110(6):2465-73.
51. Xiao SH, Catto BA, Webster LT, Jr. Effects of praziquantel on different developmental stages of Schistosoma mansoni in vitro and in vivo. J Infect Dis. 1985;151(6):1130-7.
52. Aragon AD, Imani RA, Blackburn VR, Cupit PM, Melman SD, Goronga T, et al. Towards an understanding of the mechanism of action of praziquantel. Molecular and biochemical parasitology. 2009;164(1):57-65.
53. Masi B, Perles-Barbacaru TA, Bernard M, Viola A. Clinical and Preclinical Imaging of Hepatosplenic Schistosomiasis. Trends Parasitol. 2020;36(2):206-26.
54. Li-zhi W, Xin-Sheng Z, Jiang-shan D, Yi W, Bao-an Y. Transdermal praziquantel administration attenuates hepatic granulomatosis in mice infected with Schistosoma japonicum. Parasitology research. 2015;114(4):1417-24.
55. Breiser A, Kim DJ, Fleer EA, Damenz W, Drube A, Berger M, et al. Distribution and metabolism of hexadecylphosphocholine in mice. Lipids. 1987;22(11):925-6.
56. Jimenez-Anton MD, Garcia-Calvo E, Gutierrez C, Escribano MD, Kayali N, Luque-Garcia JL, et al. Pharmacokinetics and disposition of miltefosine in healthy mice and hamsters experimentally infected with Leishmania infantum. European journal of pharmaceutical sciences : official journal of the European Federation for Pharmaceutical Sciences. 2018;121:281-6.
57. Morsy G. Parasitological and histo-pathological studies on schistosomiasis mansoni infected mice and treated with praziquatel and/or oltipraz. Journal of the Egyptian Society of Parasitology. 2009;39(2):687-701.
58. Xiao S, Binggui S, Chollet J, Tanner M. Tegumental changes in 21-day-old Schistosoma mansoni harboured in mice treated with artemether. Acta tropica. 2000;75(3):341-8.
59. Hegazy LAM, Motiam MHA, Abd El-Aal NF, Ibrahim SM, Mohamed HK. Evaluation of Artesunate and Praziquantel Combination Therapy in Murine Schistosomiasis mansoni. Iran J Parasitol.

2018;13(2):193-203.
60. Gouveia MJ, Brindley PJ, Azevedo C, Gartner F, da Costa JMC, Vale N. The antioxidants resveratrol and N-acetylcysteine enhance anthelmintic activity of praziquantel and artesunate against Schistosoma mansoni. Parasites & vectors. 2019;12(1):309.
61. Yepes E, Varela MR, Lopez-Aban J, Rojas-Caraballo J, Muro A, Mollinedo F. Inhibition of Granulomatous Inflammation and Prophylactic Treatment of Schistosomiasis with a Combination of Edelfosine and Praziquantel. PLoS neglected tropical diseases. 2015;9(7):e0003893.
62. El-Refai SA, Atia AF, Mahmoud SF. Effects of Callistemon citrinus aqueous extract on prepatent and patent infections with Schistosoma mansoni in experimentally infected mice. J Helminthol. 2019;93(4):424-33.
63. Ghosh S, Ghosh S, Sil PC. Role of nanostructures in improvising oral medicine. Toxicol Rep. 2019;6:358-68.

Tables

Table 1 Effect of PZQ-MFS nanocombinations on worm burden in comparison with nontreated and respective monotherapy controls

Subgroup / Stage	Non treated (NT) control	Worm burden and percent reduction (% R) (Group I) Higher dose LNCs			(Group II) Lower dose LNCs			F(p)
		Subgroup Ia 250 mg/kg PZQ	Subgroup Ib 20 mg/kg MFS	Subgroup Iab 250 mg/kg PZQ-20 mg/kg MFS	Subgroup IIa 125 mg/kg PZQ	Subgroup IIb 10 mg/kg MFS	Subgroup IIab 125 mg/kg PZQ-10 mg/kg MFS	
Invasive (1)								
Mean ± SD.	38.83 ± 1.17	11.0 ± 2.61	9.17 ± 2.93	6.17 ± 1.47	17.33 ± 3.14	30.50 ± 4.04	15.50 ± 1.87	124.405* (<0.001*)
% R		71.67	76.39	84.12	55.36	21.46	60.09	
p_0		<0.001*	<0.001*	<0.001*	<0.001*	<0.001*	<0.001*	
Significance		p_1=0.887, p_2=0.044*, p_3=0.449, p_4<0.001*, p_5=0.887, p_6<0.001*, p_7<0.001*						
Juvenile (2)								
Mean ± SD.	38.83 ± 1.17	29.33 ± 2.50	3.17 ± 1.17	3.0 ± 0.89	29.83 ± 3.66	19.50 ± 1.87	21.0 ± 3.90	185.422* (<0.001*)
% R		24.46	91.85	92.27	23.18	49.79	45.92	
p_0		<0.001*	<0.001*	<0.001*	<0.001*	<0.001*	<0.001*	
Significance		p_1<0.001*, p_2<0.001*, p_3=1.000, p_4<0.001*, p_5<0.001*, p_6=0.935, p_7<0.001*						
Adult (3)								
Mean ± SD.	38.83 ± 1.17	4.33 ± 2.25	5.17 ± 3.19	2.33 ± 1.03	12.83 ± 1.47	25.0 ± 1.41	13.0 ± 3.90	197.693* (<0.001*)
% R		88.84	86.70	93.99	66.95	35.62	66.52	
p_0		<0.001*	<0.001*	<0.001*	<0.001*	<0.001*	<0.001*	
Significance		p_1=0.995, p_2=0.739, p_3=0.356, p_4<0.001*, p_5=1.000, p_6<0.001*, p_7<0.001*						

% R: Percentage of reduction in each of the studied subgroups relative to infected non-treated control (NT)

F: F for ANOVA test, pairwise comparison between each two subgroups was done using Post Hoc Test (Tukey)

p: p value for comparing between subgroups

p_0: p value for comparing between NT control and each other subgroups

p_1: p value for comparing between Ia and Ib p_2: p value for comparing between Ia and Iab p_3: p value for comparing between Ib and Iab

p_4: p value for comparing between IIa and IIb p_5: p value for comparing between IIa and IIab p_6: p value for comparing between IIb and IIab

p_7: p value for comparing between Iab and IIab *: Statistically significant at $p \leq 0.05$

Table 2 Effect of PZQ-MFS nanocombinations on hepatic granuloma size in comparison with nontreated and monotherapy controls

Subgroup Stage	Non treated (NT) control	Hepatic granuloma size (µm) and percent reduction (% R) (Group I) Higher dose LNCs			(Group II) Lower dose LNCs			F(p)
		Subgroup Ia 250 mg/kg PZQ	Subgroup Ib 20 mg/kg MFS	Subgroup Iab 250 mg/kg PZQ-20 mg/kg MFS	Subgroup IIa 125 mg/kg PZQ	Subgroup IIb 10 mg/kg MFS	Subgroup IIab 250 mg/kg PZQ-20 mg/kg MFS	
Invasive (1)								
Mean ± SD.	412.0 ± 37.83	229.4 ± 36.77	238.3 ± 13.57	214.6 ± 18.47	303.3 ± 49.15	347.9 ± 47.24	314.5 ± 44.01	21.877* (<0.001*)
% R		↓44.33	↓42.15	↓47.92	↓26.38	↓15.55	↓23.67	
p_0		<0.001*	<0.001*	<0.001*	<0.001*	0.075	0.001*	
Significance		p_1=1.000, p_2=0.993, p_3=0.926, p_4=0.401, p_5=0.998, p_6=0.719, p_7=0.001*						
Juvenile (2)								
Mean ± SD.	412.0 ± 37.83	287.5 ± 34.46	221.9 ± 8.36	209.6 ± 21.41	378.6 ± 15.91	315.8 ± 21.02	385.4 ± 27.20	59.525* (<0.001*)
% R		↓30.22	↓46.15	↓49.13	↓8.07	↓23.34	↓6.46	
p_0		<0.001*	<0.001*	<0.001*	0.296	<0.001*	0.555	
Significance		p_1=0.002*, p_2<0.001*, p_3=0.980, p_4=0.003*, p_5=0.999, p_6=0.001*, p_7<0.001*						
Adult (3)								
Mean ± SD.	412.0 ± 37.83	230.6 ± 7.02	216.9 ± 22.30	153.5 ± 12.0	326.3 ± 38.68	336.6 ± 24.58	349.6 ± 21.26	73.989* (<0.001*)
% R		↓44.02	↓47.36	↓62.73	↓20.81	↓18.31	↓15.15	
p_0		<0.001*	<0.001*	<0.001*	<0.001*	<0.001*	0.003*	
Significance		p_1=0.966, p_2<0.001*, p_3=0.003*, p_4=0.992, p_5=0.705, p_6=0.974, p_7<0.001*						

% R: Percentage of reduction in each of the studied subgroups relative to infected nontreated control (NT)

F: F for ANOVA test, pairwise comparison between each two subgroups was done using Post Hoc Test (Tukey)

p: p value for comparing between subgroups

p_0: p value for comparing between NT control and each other subgroups

p_1: p value for comparing between Ia and Ib p_2: p value for comparing between Ia and Iab

p_3: p value for comparing between Ib and Iab

p_4: p value for comparing between IIa and IIb p_5: p value for comparing between IIa and IIab

p_6: p value for comparing between IIb and IIab

p_7: p value for comparing between Iab and IIab *: Statistically significant at $p \leq 0.05$

Figures

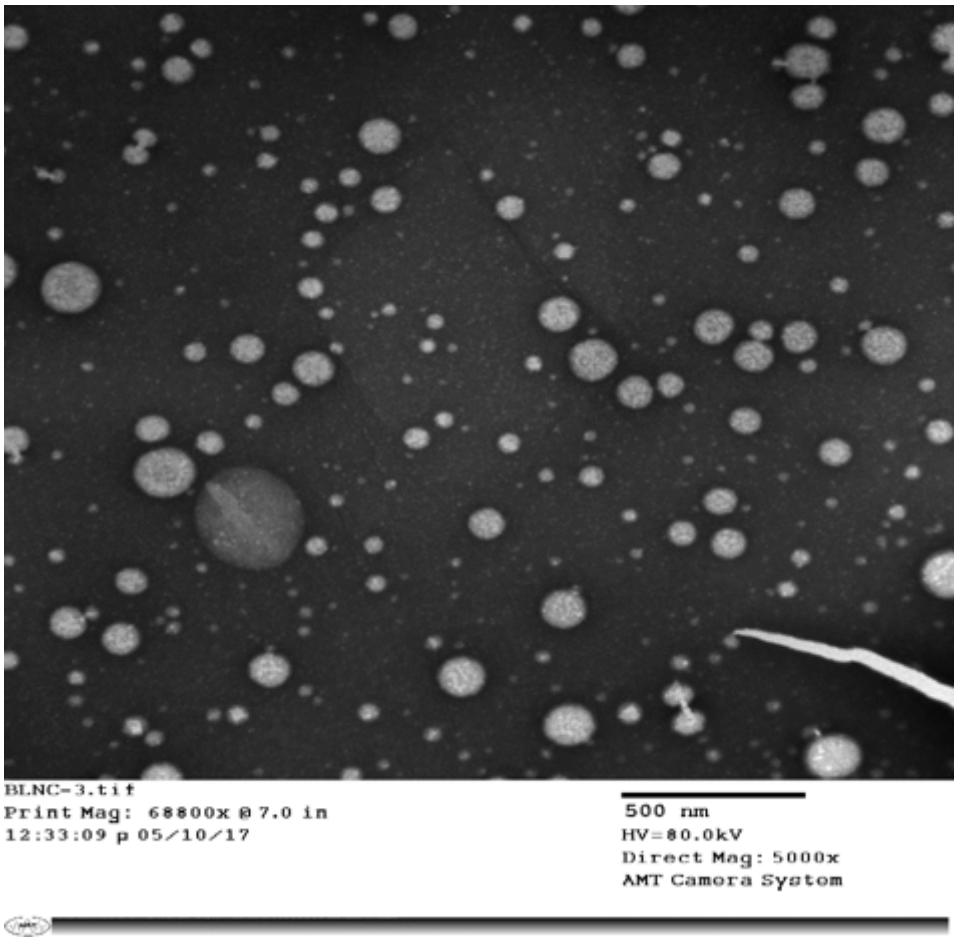

Figure 1

TEM image of praziquantel-miltefosine combination lipid nanocapsules

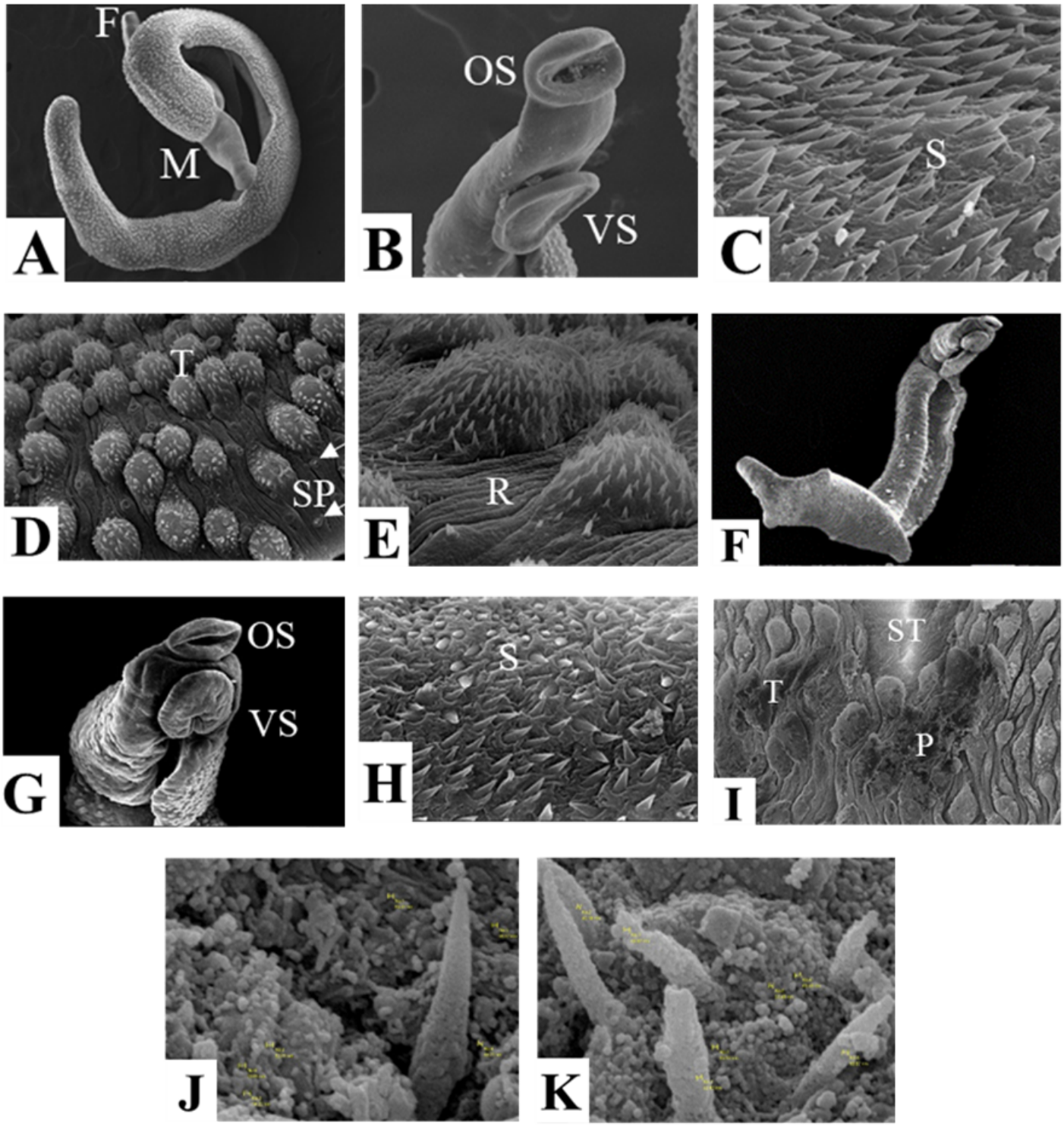

Figure 2

SEM images of S. mansoni male worms recovered from the hepatic and mesenteric veins of infected nontreated mice (Fig 2 A-E) and infected mice treated with the higher dose PZQ-MFS nanocombination (PZQ 250 mg-MFS 20 mg/kg, Subgroup Iab) (Fig 2 F-K) (A) SEM of normal male worm in copula with female (x80); (B) Normal oral and ventral suckers (x250); (C) with apically directed spines (x7000); (D) Normal dorsolateral tegument surface of the mid body showing crablike uniformly distributed tubercles

with sharp visible intact spines and sensory papillae (x1500); (E) Normal tegumental ridges between the tubercles (x4000); Adult males recovered from S. mansoni-infected mice treated with the higher fixed dose nanocombination (Subgroup Iab) (F-K) showed (F) deformed whole body (x80); (G) deformed oral and ventral suckers (x250); (H) blunt, short and loose spines (x7000); (I) extensive dorsal tegumental damage in the form of peeling of tubercles, spine disfigurement, vesicle formation and exposure of subtegumental tissue (x12000); (J & K) LNCs deposited on the damaged subtegumental tissue and the loose disfigured spines (x30000). F: female, M: male, OS: oral sucker, VS: ventral sucker, S: spine, T: tubercle, SP: sensory papillae, R: ridge, ST: subtegumental tissue, P: peeling of the tubercles.

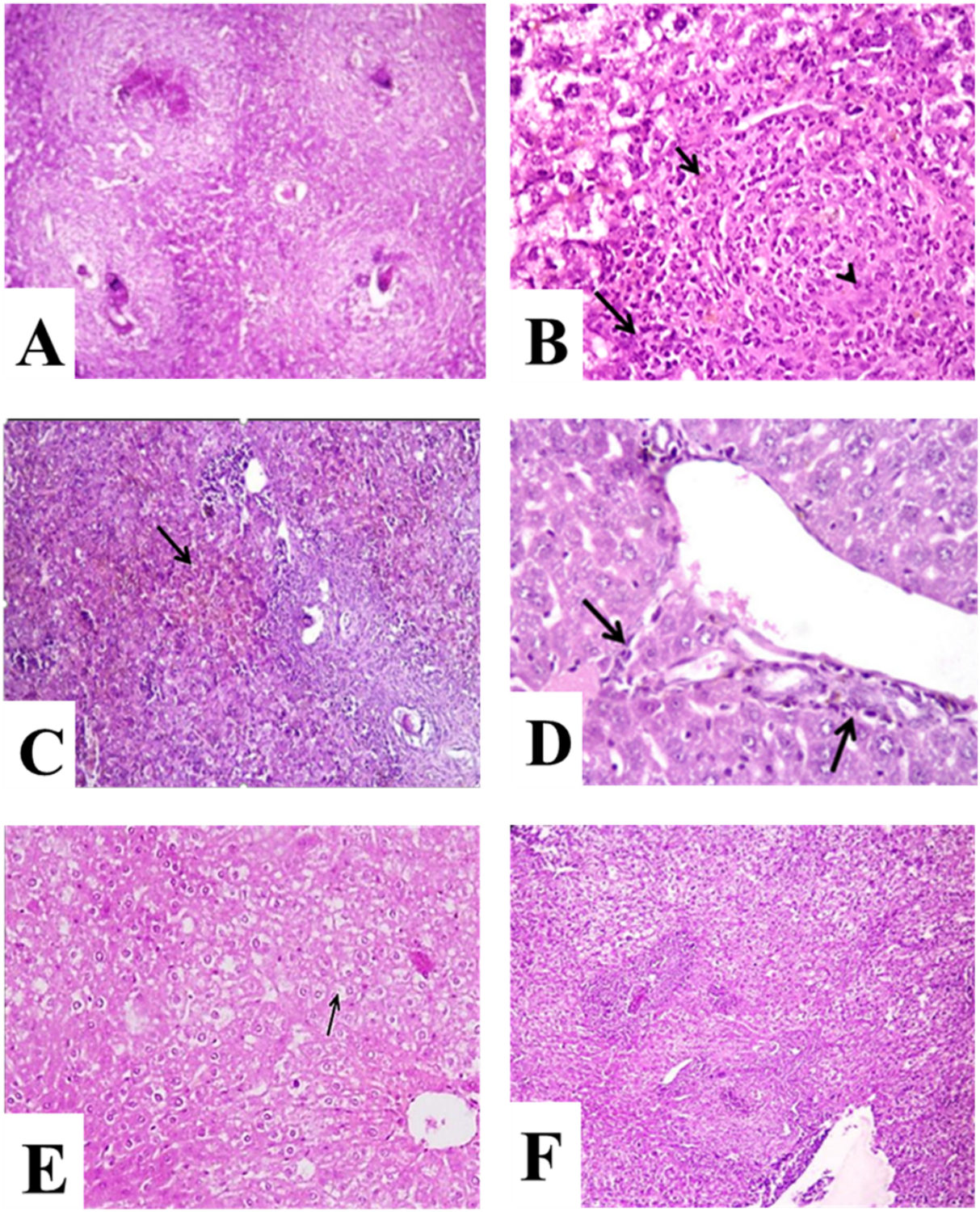

Figure 3

H&E-stained liver sections of S. mansoni-infected nontreated mice showing: (A) preserved hepatic architecture and multiple numerous closely packed necrotic and exudative-productive bilharzial granulomas (x100); (B) a granulomatous reaction formed of inflammatory cells mainly eosinophils (short arrows), neutrophils (long arrows) and histiocytes (arrow heads) (x400); (C) brownish bilharzial pigment (arrow) (x100); (D) Kupper cell hyperplasia (arrows) (x400); (E) fatty change of hepatocytes (arrow)

(x100); liver section of S. mansoni-infected mice treated with the higher dose fixed combination (Subgroup Iab) showing (F) small-sized healing granulomas (x100).